Catalysis Today 441 (2024) 114904

Contents lists available at ScienceDirect

Catalysis Today

journal homepage: www.elsevier.com/locate/cattod

The role of Cu and film thickness on the photocatalytic activity of mesoporous spin coated TiO_2 films

Samah H. Alsidran [a], Christopher Court-Wallace [a], Philip R. Davies [a,c,*], Shaoliang Guan [b,c], David J. Morgan [a,c], Genevieve Ososki [a]

[a] Cardiff Catalysis Institute, School of Chemistry, Cardiff University, CF10 3AT, UK
[b] Maxwell Centre, Cavendish Laboratory, JJ Thomson Avenue, Cambridge CB3 0HE, UK
[c] HarwellXPS, Research Complex at Harwell, Rutherford Appleton Laboratory, Harwell Science and Innovation Campus, OX11 0FA, UK

ARTICLE INFO

Keywords:
Photocatalysis
Surface
TiO_2
Spin coating

ABSTRACT

Most practical applications of photocatalysts will involve coatings on an inert support; here we have examined how copper doping of spin coated porous TiO_2 films affects their physical characteristics and photocatalytic activity. The photocatalytic degradation of stearic acid was used as a measure of photocatalytic activity for catalysts spin coated from a sol-gel onto glass with 0, 0.1, 0.5, 1, 2.5 and 5 wt% copper introduced into the catalyst lattice before gelation. The effects of spin coating speed on film thickness, structure and band gap were studied and the nature of the copper incorporated into the films examined with XPS and XANES measurements. Increased spin coating speeds reduces the thickness of the deposited films from ~ 50 μm to ~ 20 μm until a spin speed of ~ 3000 rpm at which point non-Newtonian behaviour of the gels prevents further reductions in film thickness. A larger effect on film thickness is the presence of the added copper nitrate which results in thinner films. After calcining, XANES shows the bulk of the copper to be in a Cu(II) state but at the surface of the thinnest, most active films XPS shows only Cu(I). Photocatalytic activity is much more strongly affected by the presence of the copper than the thickness of the films with 0.1 wt% Cu catalysts as much as 10 times more active than the undoped catalysts. Increasing the copper content, however, reduces activity until at ~ 5 wt% activity is lower than for the pure TiO_2 films.

1. Introduction

To date, despite an enormous body of work on alternatives, TiO_2 remains the most reliable, accessible and effective semiconductor for the photocatalytic degradation of organic molecules. Its activity under near UV light, long-term stability, low cost and ease of synthesis means TiO_2 continues to be the catalyst of choice in the research literature [1–4]. A great deal of work has focused on improving the photocatalytic activity of TiO_2, which is too low for practical applications in its natural state, and on countering the limitations of its band gap of ~ 3.2 eV which restricts the wavelengths of light for which the catalyst is effective to a small percentage of the sunlight that reaches the Earth's surface. One of the most popular strategies to address these two points has been to explore the effect of introducing additives into the TiO_2 lattice and great deal of work has been conducted into different substituents. In general, the results show that a balance needs to be found between the positive influence of additives introducing electronic states that reduce the band gap and hence the range of wavelengths captured and the negative influence of additives acting as recombination centres that shorten the lifetime of the excitons and hence the effectiveness of the catalysts. One additive that has been shown to be particularly effective is copper, although some contrary results have also been obtained [5–10]. Another strategy that has been employed to improve activity is to increase the surface area of the catalysts by introducing a degree of porosity using a variety of different strategies [6,11–13]. Combining these approaches Trofimovite et al [6]. showed that mesoporous TiO_2 powders have improved activity for the photodegradation of methyl orange and that the addition, by wet impregnation, of low loadings of copper ions also boosts performance. The copper was deemed to be present in an atomically dispersed Cu(I) state decorating the surface of the TiO_2 nanoparticles.

Practical applications of TiO_2 based catalysts will inevitably involve thin coatings deposited on inert high area supports, and sol gel based preparations have received a great deal of attention in this respect

* Corresponding author at: Cardiff Catalysis Institute, School of Chemistry, Cardiff University, CF10 3AT, UK.
E-mail address: daviespr@cardiff.ac.uk (P.R. Davies).

https://doi.org/10.1016/j.cattod.2024.114904
Received 29 April 2024; Received in revised form 5 June 2024; Accepted 18 June 2024
Available online 19 June 2024

because of their ease of preparation, and the fact that most fundamental research laboratories are able to create TiO_2 films from sol-gels at minimal cost and on short time scales. Three main approaches have been considered: dip coating, spin-coating and spray deposition [14]. Of the three, spin coating has the advantage of high reproducibility, rapid preparation of large areas and readily controllable film thicknesses using deposition spin speeds between 500 and 8000 rpm, and in the present study we have used this approach to explore how copper doping, film thickness and porosity influence the activity of TiO_2 films. We find that the increased activity due to porosity is maintained when the coatings are deposited on silica surfaces and that Cu(I) ions within the lattice at low concentrations are key to increasing activity.

2. Experimental

Titanium (IV) butoxide ($Ti(OBu)_4$, Sigma-Aldrich reagent grade) was used as a precursor with methanol as a solvent. The procedure for developing a mesoporous structure using pluronic P-123 (Sigma-Aldrich) was optimised in terms of quantities of templating agent, stirring times and annealing temperatures [15]. For all the samples reported here, 5 g pluronic P-123 was added to 15 cm^3 methanol (Sigma Aldrich, anhydrous 99.8 %) and left to stir until the polymer was fully dissolved whereupon 10 cm^3 $Ti(OBu)_4$ was added and the solution left to stir for 30 minutes in a dry atmosphere since hydrolysis from the air has been shown to have a detrimental effect on the quality and activity of the porous films deposited by spin coating [15]. Cover glasses (VWR, 22 mm Ø, No. 1) were cleaned in water, then acetone using an ultrasonic bath at room temperature and placed in an oven at 40 °C. The titanium butoxide solution was distributed onto the clean cover slips by spin coating with a Laurell, WS-650MZ-23NPP system. 200 μl of the titanium butoxide solution was dispensed onto a spinning cover glass, the coated cover glass was left to spin for a further 30 seconds. Spin speeds between 500 – 8000 rpm were used to achieve differing film thicknesses. The samples were then heated to 40 °C for 48 hours to facilitate the evaporation-induced self-assembly of the polymer and create a porous structure after which the samples were calcined in the furnace at 500 °C for 5 hours with a heating rate of 5 °C min^{-1} to remove the templating polymer. Control samples in which pluronic acid was included but the evaporation-induced self-assembly of the polymer inhibited by low temperatures (21 °C) or prevented entirely by calcining immediately after spin coating show correspondingly low reaction rates.

2.1. Film thickness measurement & dependence on experimental parameters

Film thicknesses were measured using a Sensofar "S mart" optical profilometer by scraping off a section of the film using a plastic glue spreader, creating a step between the uncoated glass coverslip and the photocatalytic coating. 3D profiles were measured at multiple points across the threshold between the two surfaces as well as the intact central portion and edge of each sample, thickness measurements were within ~ 10 % across a sample. All the spin coated films were discontinuous on the silica substrates, Figure SI-1, but remarkably similar to each other at different spin speeds. There is very little variation in the depth or width of the channels in the surface, with the deepest measuring approximately 1.5 μm deep and average channel widths at their mid points ranging from ~12 μm at lower spin speeds, to ~15 μm for preparation spin speeds between 4500 and 8000 rpm.

2.2. Photocatalytic testing

The photoactivity of the films was monitored by measuring the surface concentration of C-H bonds of a stearic acid film using diffuse reflectance infrared Fourier-transform spectroscopy (DRIFTS) on a Perkin Elmer Frontier spectrometer [16]. 200 μL of 0.1 mol dm^{-3} stearic acid (Sigma Aldrich, reagent grade, 95 %) in chloroform (reagent grade) was spin coated on to the photocatalytic films at 2000 rpm for 30 s. During deposition, the chloroform is completely desorbed, with no trace of chlorine seen in the XPS of deposited acid. Samples were illuminated with an adapted UV-LED based photocatalytic test reactor developed as part of the EU funded PCATDES project, providing a calibrated adjustable light source with a light intensity of up to 1.9 kW m^{-2} at a wavelength of 365 ± 2 nm at a distance of 0.1 m from the UV-LEDs [17,18]. The films were positioned c.a. 10 cm from the LED source and photocatalysis conducted in air. No temperature change was detected in the samples during photocatalysis.

All measurements are an average of at least three experiments on different batches of the same nominal material; the narrow error range measured demonstrates the excellent reproducibility of the coating and reaction procedures. The percentage of stearic acid decomposed was calculated from the combined peak areas under the C-H absorption peaks at 2917 cm^{-1} and 2849 cm^{-1} after subtraction of a constant background using OriginLab software.

2.3. Catalyst characterisation

DRS-UV spectroscopy was performed using an Agilent Technologies Cary Series UV-Vis spectrometer scanning from 800 to 200 nm. XP spectra were obtained of the coatings with a ThermoFisher Scientific K-Alpha$^+$ photoelectron spectrometer, utilising micro-focussed monochromatic Al kα radiation with a photon energy of 1486.6 eV and operating at 72 W (6 mA × 12 kV). Spectra were collected using the 400-micron spot mode which averages the signal from an area of *ca.* 600×400 microns. A pass-energy of 40 eV was used for high-resolution scans and 150 eV for survey scans with 0.1 eV and 1.0 eV step sizes respectively. Depth profiling was performed with argon clusters of approximately 2000 atoms, from a Thermo MAGCIS source operating at 4 kV and rastered over a 2×1 mm area for a period of 30 seconds per cycle. CasaXPS [19,20] (version 2.3.24) was used to analyse the spectra using Shirley type backgrounds and Scofield cross sections with an energy dependence of −0.6. Binding energies are referenced to the largest Al^{4+} (2p) peak at 458.5 eV with an uncertainty of ~ 0.2 eV.

Powder X-ray diffraction (XRD) data over the range 2θ = 10–80°, Figure SI-2, were obtained using a PANalytical X'Pert Pro diffractometer with a monochromatic Cu Kα source ($\lambda = 0.154$ nm) operated at 40 kV and 40 mA.

Surface area was measured using a Quantachrome NOVA 4200e instrument by N_2 adsorption using NovaWin v11.03 analysis software. Samples were degassed under vacuum at 150 °C for 2.5 hours. Adsorption/desorption isotherms were recorded at −196 °C. BET surface areas were calculated over the relative pressure ranges 0.05–0.2 and 0.06–0.3 for the non-porous and porous samples respectively. The catalyst precursor solutions were prepared in the same way as for the spin coated films but then transferred to crucibles, warmed to 40 °C for 48 hours before calcining at 500 °C for 5 hours at a heating rate of 5 °C min^{-1}. The resulting powders were then ground to form free flowing powders.

3. Results and discussion

3.1. The effect of added porosity on photocatalytic activity in spin coated films

To confirm that the porosity introduced into the TiO_2 materials with a templating polmer [6] is maintained in the spin coated and calcined films, the activity of a range of films deposited at different spin speeds was compared, Fig. 1a). In this Figure the % of stearic acid removed by oxidation over the film is plotted against time of exposure to UV light; the porous films all fall within a range highlighted in green that is approximately 10× faster than that of the non-porous films which lie in a range highlighted in blue. The increase in rate that is evident when porosity is introduced is far in excess of the ~2× increase in surface

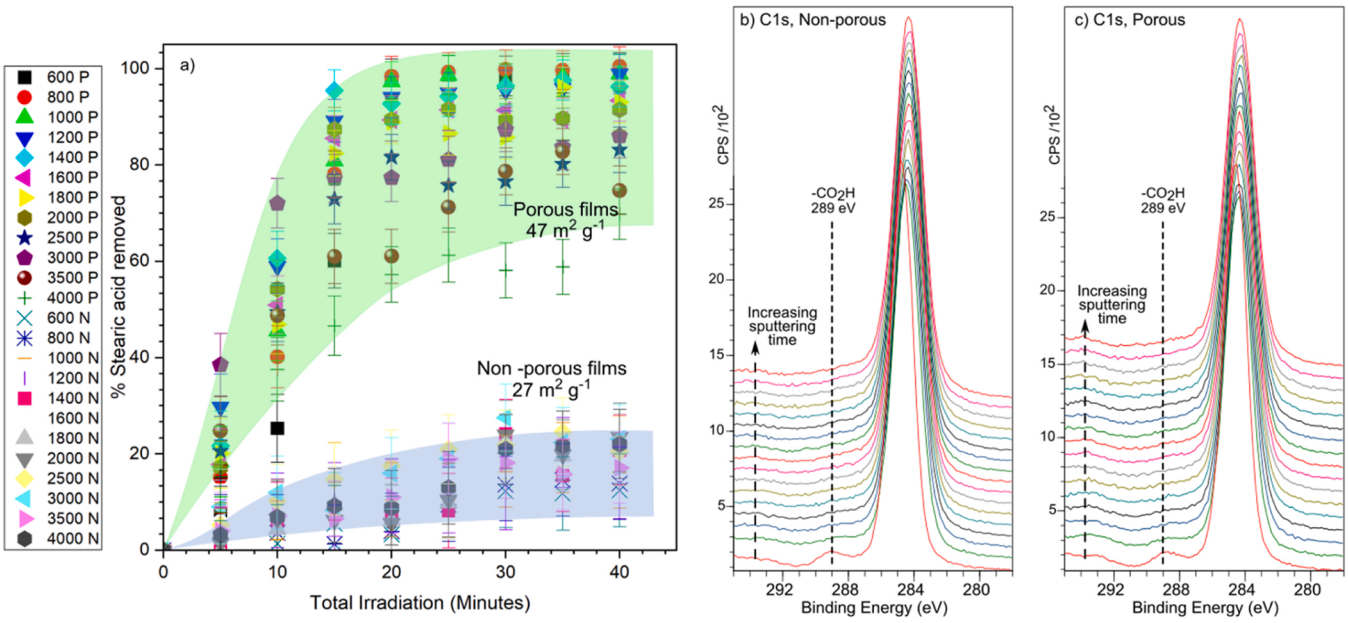

Fig. 1. a) Comparison of the photocatalytic performance of a selection of porous and non-porous TiO_2 films (without copper) spin-coated at different speeds. Deposition spin speeds are listed in the figure legend in rpm; P & N indicate porous and non-porous films respectively. Typical surface areas of the films (scraped off the glass substrate) are also given. The increased rate of reaction (up to 10× faster) of the porous films is much greater than could be accounted for by the increased surface area. b) & c) XPS depth profiling of porous and non-porous films using a cluster argon etch between scans. The carboxylic carbon signal at 289 eV vanishes after the first etch in both the porous and non-porous coatings suggesting no difference in the depth to which the acid diffuses into the catalyst.

area. Interestingly, XPS depth measurement profiling, Fig. 1b) & c), don't show any differences in the penetration of the acid between the porous and non-porous films. In both cases, the presence of the carboxylic head group is only detected in the very top layer. This suggests that the difference in activity is not connected with the transport of the target molecule (stearic acid in this case) into the pores created by the templating polymer but perhaps more with the transport of the other reactants (water and oxygen) to the active site. We have not explored this interesting observation any further in this work, focussing instead on how porous films are affected by copper doping and deposition spin speed. The catalysts show excellent re-usability, with ~ 93 % activity retained over 4 reaction cycles, Table SI-1.

3.2. The effect of Cu doping on the activity of porous spin coated TiO_2 films

Copper doping is a well-known means of increasing the activity of TiO_2 photocatalysts [1,5,6,10,21,22] and in our investigation reported here, the porous thin films are no exception. Fig. 2 shows the effect of a selection of copper loadings on the activity of TiO_2 films spin coated at 3000 rpm; strikingly, at the highest concentration of copper (5 wt%) the films are significantly less active than the undoped samples, but activity increases as the Cu wt% decreases. Previously, Zhang et al. reported [21] an optimum Cu doping level of ~1.6 wt% for sputter coated TiO_2 films, and Trofimovaite reported [6] increased activity with Cu concentrations below 0.8 wt% whereas Krishnakumar et al. reported enhanced activity of a TiO_2 powder synthesised with approximately 4 wt% of Cu, slightly decreasing at Cu contents of 7 and 11 wt%. In contrast, Colon et al. report a decrease in activity for TiO_2 catalysts with ~ 0.6 and 1.1 wt% Cu although catalysts prepared in the presence of sulfuric acid was enhanced.

It's also noticeable that the 0.1 and 5 wt% curves are very close to linear indicating zero order kinetics as expected for this reaction where sites are likely to be initially saturated [23], whereas the 0, 0.5 and 2.5 wt% curves show some dependence on concentration and can be fitted by 1st order curves. We do not, at present, have an explanation for the different behaviours but for this reason, rates in this paper are

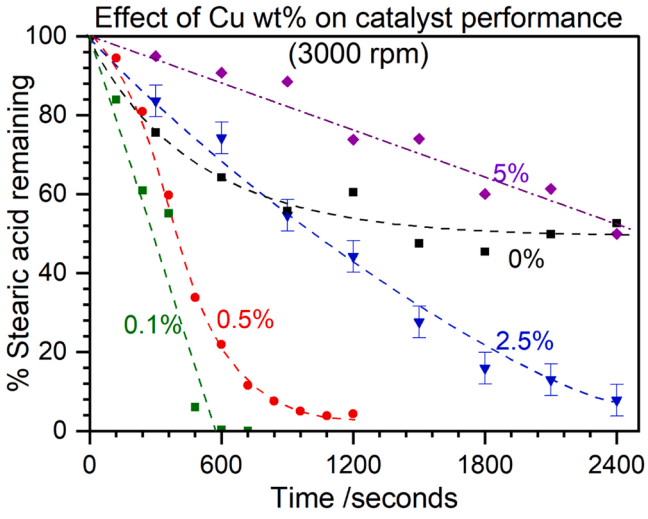

Fig. 2. Effect of Cu loading (0, 0.1, 0.5, 2.5 & 5 wt%) on the activity of porous TiO_2 films deposited at a spin speed of 3000 rpm. To reduce the clutter in the chart, errors in the measurements are indicated on only one of the curves but were similar for all the data.

considered in terms of half-lives so that similar units are involved with every film studied.

XRD patterns of the samples, Figure SI-2 show only the TiO_2 reflections expected for anatase, together with broad peaks at 2θ of 16°, 22.8° and 34.8° for the thinner films deposited at higher spin speeds, which are attributed to glass shards scraped off the cover slip support. There is no evidence for the presence of either cupric or cuprous oxide implying that the copper is either incorporated into the TiO_2 lattice as has been reported previously or that it forms amorphous or very small (< 5 nm) nanoparticles.

XP spectra of the films, Fig. 3a), show that at higher concentrations the majority of copper in the surface and near-surface region is in a Cu

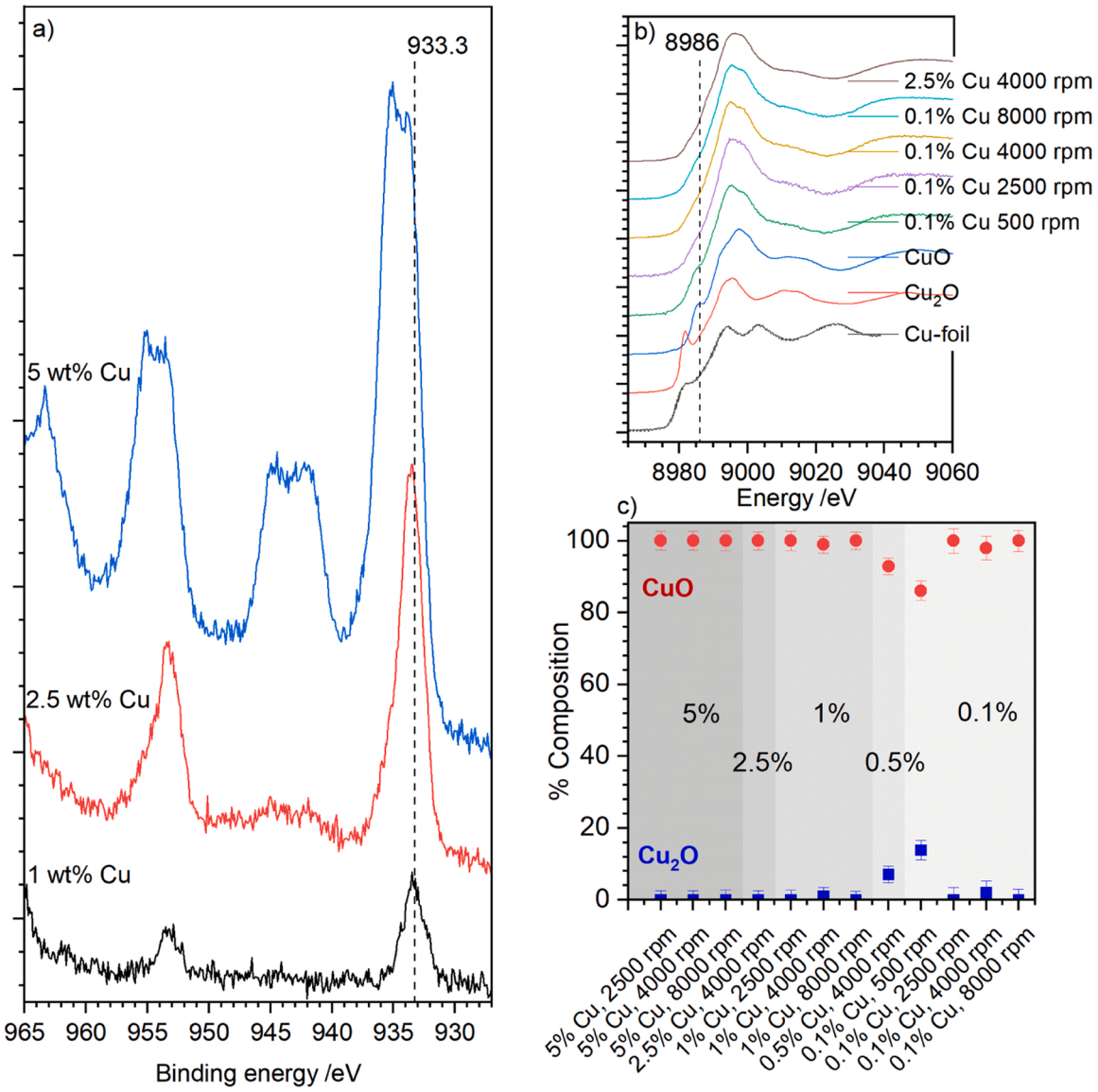

Fig. 3. Characterisation of the oxidation state of copper doped into TiO_2. a) XP spectra of copper doped TiO_2 films.; b) XANES spectra of the Cu edge comparing the doped TiO_2 films with copper ions in Cu metal, Cu_2O and CuO standards; c) % composition of the bulk of the samples calculated from a deconvolution of the XANES data.

(II) oxidation state but at low concentrations, it is in either the Cu(I) or Cu(0) state. Reduction under the x-rays was ruled out by studying the films before and after exposure to the x-rays over ~ 40 minutes which showed no significant change to the Cu 2p peaks. Whilst the Cu Auger peak is too weak to definitively differentiate between the 0 and +1 oxidation states in our catalysts, the likelihood is that Cu(I) is present in the oxidative environment and this is consistent with Tseng et al.'s study of Cu/TiO_2 sol gel synthesis [24] where Cu(I) was the dominant copper species at the surface. The assignment to Cu(I) is confirmed by the XANES measurements which show no evidence of Cu(0), they also show that in contrast to the copper species in the surface region, the ions in the *bulk* of the TiO_2 are predominantly Cu(II), only at the lowest Cu concentration do Cu(I) states make any significant contribution to the total. An interesting point is a lower intensity of the pre-edge feature in the Cu (I) when incorporated into the TiO_2 lattice compared with the Cu_2O standard. The data in Trofimovaite et al.'s paper shows similar behaviour which they concluded indicated the presence of Cu(I) in environments structurally similar to those in mononuclear complexes. Kau et al. reported a very detailed study of the Cu(I) edge feature and showed that the intensity of this feature is diminished in compounds with higher symmetry coordinations.

These results are also consistent with the view expressed by both Colon et al. [10], and Gray et al [22]. that Cu(II) states are detrimental for photocatalytic processes, acting as recombination centres whereas Krishnakumar et al. suggested that increased activity could be ascribed to Cu(II) states creating oxygen vacancies in the TiO_2 lattice. Tseng et al. [24], studied the effect of Cu/TiO_2 photocatalysts on the photoreduction of CO_2 and noted an enhancement with the presence of Cu_2O. More recently, a study by Abegão [5] proposed that Cu(II) ions are essential for the photocatalytic reduction of CO_2 but they have only looked at relatively high wt% loadings. Our data suggests that the presence of Cu (II) does not enhance photocatalytic activity, rather it is conditions where the Cu(I) state dominates that seem to be associated with highest activity.

3.3. *The effect of Cu doping on spin coating film thickness*

Spin coating is a well-established, and highly reproducible method of creating uniform films with well controlled thicknesses. For a Newtonian fluid, the film thickness is expected to decrease with the square root

of the angular velocity [25,26]. However, suspensions containing dissolved polymers commonly exhibit non Newtonian behaviour due to shear thickening effects and this behaviour was observed for all the coatings examined in this study. At low speeds, where shear forces are too weak to influence the coating, the expected dependence of thickness on spin speed is observed but this changes abruptly for all the samples with a spin speed being reached at which the film thickness is almost independent of deposition speed. A "critical shear rate" can be estimated from the intercept of a linear extrapolation of the two states; this is illustrated for a the 0, 0.1 and 5 wt% Cu doped films in Fig. 4 and summarised in Table 1 for different Cu concentrations. It is evident that the presence of copper ions within the precursor solution reduces the critical shear rate of the solution and hence film thickness, reducing the thickness of the films formed. This can be attributed to an inhibiting effect of the copper ions on the hydrolysis of the titanium butoxide, reducing the viscosity of the solutions which results in a reduction in the critical sheer rate spin speed.

All the films generated by spin coating show cracking in the calcined film however, the coating morphology was not affected by the spin speed or by Cu doping. Figure SI-1 for example shows a set of line profiles recorded using optical profilometry, across a range of spin speeds for a 1 wt% Cu doped film demonstrating the high level of consistency across the range studied. The photocatalytic activity variation discussed below is not therefore due to differences in the morphology of the films.

3.4. Effect of deposition conditions on the photocatalytic activity of spin coated films

Plotting the half life of the photocatalytic decomposition reaction in the absence of copper doping against spin speed suggests some correlation between the deposition conditions and a film's activity, with a slight maximum at ~ 3000 rpm, Fig. 5a. A similar trend exists for the 0.1 wt% doped sample; however, it is clear from the summary of data that it is the extent of copper doping that most strongly influences the rate of photocatalytic decomposition of stearic acid on the TiO_2 films. Band gap measurements of a selection of films, Figure SI-3, show the pure TiO_2 and 0.1 wt% doped films have close to the expected TiO_2 band gap of 3.2 eV for with no variation at different spin speeds, however the 5 wt% Cu doped samples exhibit significantly lower band gaps, that decrease further with decreasing spin speed. Since we are using a single wavelength of light (365 nm), to excite the samples, the change in band gap of our catalysts cannot benefit the activity of the films. The decrease in activity that is observed suggests that the copper ions in the samples are acting as recombination points for the electron/hole pairs.

Plotting the half-lives against measured film thickness confirms a trend of increased photocatalytic reaction rate for thinner films but its noticeable that for the thinnest films there is a spread of activities which was not apparent when plotted against spin speed. As noted above, copper doping affects both the film thickness and the photocatalytic activity of the deposited films but Fig. 5b) demonstrates that it is the Cu doping level that has the most significant effect on the photocatalytic activity, 0.1 and 0.5 wt% Cu films have consistent rates for a small range of film thicknesses whereas the undoped films and the 1 and 5 wt% Cu doped films have much lower activities even at comparable film thicknesses of ~ 15 μm.

Table 1
Dependence of critical sheer rate on the concentration of copper in the coating solution.

Copper doping:	Undoped	0.1 wt %	0.5 wt %	1 wt %	2.5 wt %	5 wt %
Critical shear rate (rpm)	2930	2894	2065	1890	2324	1527

4. Conclusions

In a thorough examination of the effect of Cu doping and deposition conditions on the photocatalytic activity of spin-coated porous TiO_2 films, we have shown that the porosity of the films is maintained with deposition and can increase the rate of photocatalytic degradation of stearic acid by a factor of up to ×10. Depth profiling data from XPS shows that even in the porous films the stearic acid doesn't penetrate far below the surface region and therefore transport of the oxidant to the reaction site is the most likely explanation for the increased rate of degradation. Deposition spin speed and hence film thickness has very little influence on the activity of the films, instead, the largest influence on activity is the extent of copper doping. Films with Cu concentrations of between ~ 0.1 wt% and 0.5 wt% are much more active than undoped films but this activity decreases as the copper level is increased and by 5 wt% Cu the activity is lower than that of the pure TiO_2. The high activity of the films appears to be associated with Cu(I) states in the surface region of the films although XANES data strongly suggests that the oxidation state of the majority of the copper in the bulk of the coatings is Cu(II). The results suggest that an effective strategy for creating practical photocatalysts can ignore the thickness of the coated films and concentrate on the robustness of the catalyst and the incorporation of a promoter such as copper.

CRediT authorship contribution statement

Samah H. Alsidran: Investigation. **Genevieve Ososki:** Methodology, Investigation, Data curation. **David J. Morgan:** Writing – review & editing, Investigation, Formal analysis. **Shaoliang Guan:** Writing – review & editing, Investigation, Formal analysis. **Christopher Court-**

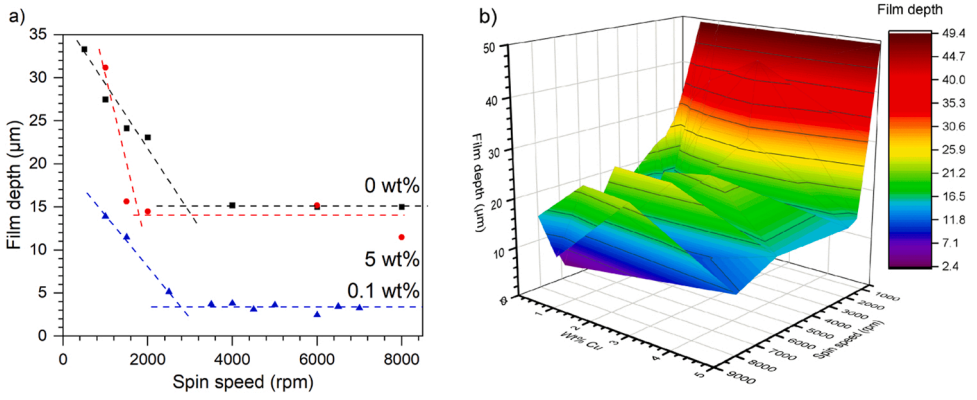

Fig. 4. a): Plot of measured thickness against spin speed for three Cu doping levels showing the change from Newtonian behaviour and the determination of the critical film sheer rate. b): Spin speed vs thickness for all the films studied.

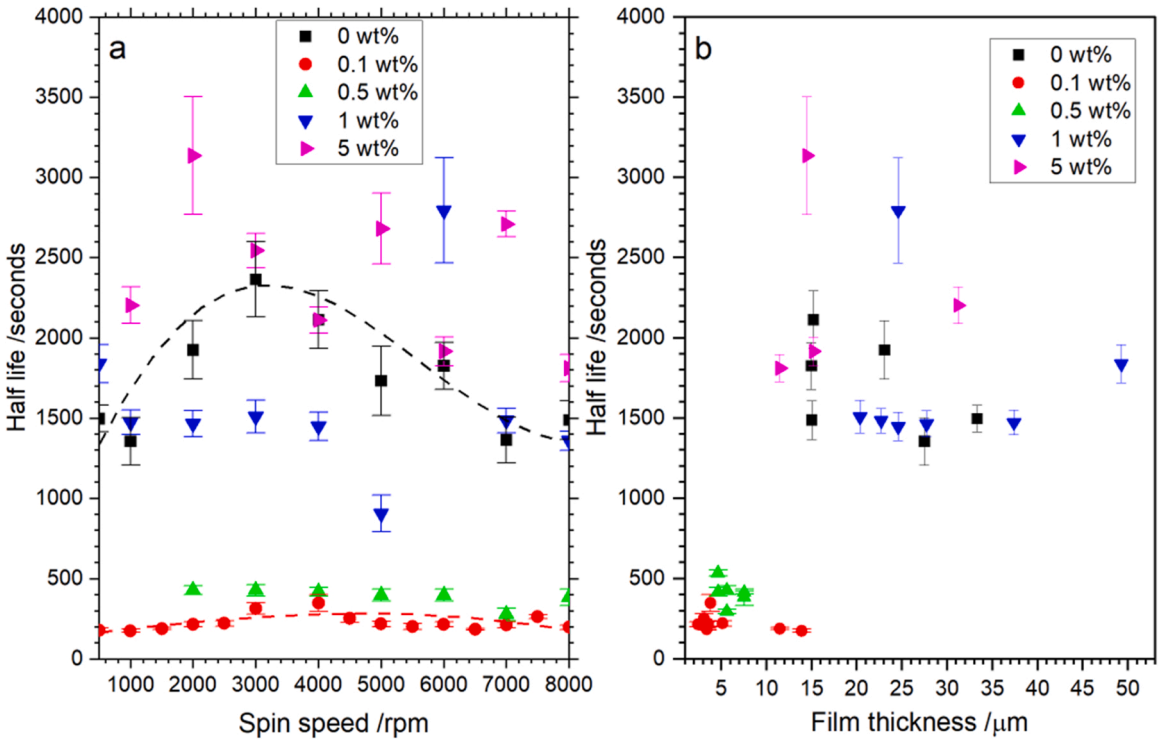

Fig. 5. Rates of reaction on doped and undoped films expressed as reaction half lives to allow comparison between reactions with different reaction rate orders. a) Comparison of half lives for selected films plotted against deposition spin speed. Curves for 0 wt% and 0.1 wt% Cu data are only to guide the eye; b) half lives plotted against measured film thickness.

Wallace: Investigation. **Philip R. Davies:** Writing – review & editing, Writing – original draft, Supervision, Resources, Project administration, Funding acquisition, Formal analysis, Data curation, Conceptualization.

Declaration of Competing Interest

The authors declare the following financial interests/personal relationships which may be considered as potential competing interests: Philip R. Davies reports financial support was provided by Engineering and Physical Sciences Research Council. If there are other authors, they declare that they have no known competing financial interests or personal relationships that could have appeared to influence the work reported in this paper.

Data availability

All data shown in this paper is available at http://doi.org/10.17035/d.2024.0325372343.

Acknowledgements

GO thanks the School of Chemistry at Cardiff University for a studentship. We are grateful to the Catalysis Hub Bag access scheme, and Drs Nitya Ramanan and Veronica Celorrio in particular, for help in acquiring the XANES spectra at the Diamond Lightsource. X-ray photoelectron (XPS) data were acquired at the EPSRC National Facility for XPS ("HarwellXPS", EP/Y023587/1, EP/Y023609/1, EP/Y023536/1, EP/Y023552/1 and EP/Y023544/1) SHA is grateful to the Government of Saudi for a scholarship grant.

Appendix A. Supporting information

Supplementary data associated with this article can be found in the online version at doi:10.1016/j.cattod.2024.114904.

References

[1] V. Kumaravel, S. Mathew, J. Bartlett, S.C. Pillai, Appl. Catal. B Environ. 244 (2019) 1021–1064.
[2] K. Hashimoto, H. Irie, A. Fujishima, Jpn. J. Appl. Phys. Part 1 Regul. Pap. Short. Notes Rev. Pap. 44 (2005) 8269–8285.
[3] M.R. Hoffmann, S.T. Martin, Wonyong Choi, D.W. Bahnemann, Chem. Rev. 95 (1995) 69–96.
[4] J.-M. Herrmann, Top. Catal. 34 (2005) 49–65.
[5] A. Adamu, M. Isaacs, K. Boodhoo, F.R. Abegão, J. CO2 Util. 70 (2023) 102428.
[6] R. Trofimovaite, C.M.A. Parlett, S. Kumar, L. Frattini, M.A. Isaacs, K. Wilson, L. Olivi, B. Coulson, J. Debgupta, R.E. Douthwaite, A.F. Lee, Appl. Catal. B Environ. 232 (2018) 501–511.
[7] F. Bensouici, M. Bououdina, A.A. Dakhel, R. Tala-Ighil, M. Tounane, A. Iratni, T. Souier, S. Liu, W. Cai, Appl. Surf. Sci. 395 (2017) 110–116.
[8] V. Krishnakumar, S. Boobas, J. Jayaprakash, M. Rajaboopathi, B. Han, M. Louhi-Kultanen, J. Mater. Sci. Mater. Electron. 27 (2016) 7438–7447.
[9] T. Aguilar, J. Navas, R. Alcántara, C. Fernández-Lorenzo, J.J. Gallardo, G. Blanco, J. Martín-Calleja, Chem. Phys. Lett. 571 (2013) 49–53.
[10] G. Colón, M. Maicu, M.C. Hidalgo, J.A. Navío, Appl. Catal. B Environ. 67 (2006) 41–51.
[11] D.M. Antonelli, J.Y. Ying, Angew. Chem. Int. Ed. Engl. 34 (1995) 2014–2017.
[12] C.-K. Tsung, J. Fan, N. Zheng, Q. Shi, A.J. Forman, J. Wang, G.D. Stucky, Angew. Chem. Int. Ed. 47 (2008) 8682–8686.
[13] W. Zhou, F. Sun, K. Pan, G. Tian, B. Jiang, Z. Ren, C. Tian, H. Fu, Adv. Funct. Mater. 21 (2011) 1922–1930.
[14] S. Obregón, V. Rodríguez-González, J. Sol. -Gel Sci. Technol. 102 (2022) 125–141.
[15] G. Ososki, PhD Thesis, Cardiff University, 2022..
[16] A. Mills, J. Wang, J. Photochem. Photobiol. Chem. 182 (2006) 181–186.
[17] A. Sergejevs, C.T. Clarke, D.W.E. Allsopp, J. Marugan, A. Jaroenworaluck, W. Singhapong, P. Manpetch, R. Timmers, C. Casado, C.R. Bowen, Photochem. Photobiol. Sci. 16 (2017) 1690–1699.
[18] C. Casado, R. Timmers, A. Sergejevs, C.T. Clarke, D.W.E. Allsopp, C.R. Bowen, R. van Grieken, J. Marugán, Chem. Eng. J. 327 (2017) 1043–1055.
[19] N. Fairley, CasaXPS Manual: 2.3.15 Spectroscopy, Casa Software Ltd, 2009.
[20] N. Fairley, V. Fernandez, M. Richard-Plouet, C. Guillot-Deudon, J. Walton, E. Smith, D. Flahaut, M. Greiner, M. Biesinger, S. Tougaard, D. Morgan, J. Baltrusaitis, Appl. Surf. Sci. Adv. 5 (2021) 100112.
[21] W. Zhang, Y. Li, S. Zhu, F. Wang, Catal. Today 93–95 (2004) 589–594.
[22] G. Li, N.M. Dimitrijevic, L. Chen, T. Rajh, K.A. Gray, J. Phys. Chem. C. 0 (2008), 0–0.
[23] S. Alofi, C. O'Rourke and A. Mills, *Photochem. Photobiol. Sci.*, doi:10.1007/s43630-022-00278-0.

[24] I.-H. Tseng, W.-C. Chang, J.C.S. Wu, Appl. Catal. B Environ. 37 (2002) 37–48.
[25] D. Meyerhofer, J. Appl. Phys. 49 (1978) 3993–3997.
[26] S.A. Jenekhe, S.B. Schuldt, Ind. Eng. Chem. Fundam. 23 (1984) 432–436.